ICAS Paper No. 68-18

GAS DYNAMICAL PHENOMENA ON ATMOSPHERIC FLIGHT VEHICLES INVOLVED IN RE-ENTRY FLIGHT

by

Jiro Kondo
Department of Aeronautics
University of Tokyo
Tokyo, Japan

The Sixth Congress of the International Council of the Aeronautical Sciences

DEUTSCHES MUSEUM, MÜNCHEN, GERMANY/SEPTEMBER 9-13, 1968

Preis: DM 2.00

GAS DYNAMICAL PHENOMENA ON ATOMOSPHERIC FLIGHT VEHICLES INVOLVED IN THE RE-ENTRY FLIGHT

Jiro Kondo
Professor, D. Sc.
University of Tokyo, Tokyo

Abstract

One of the most important aerodynamical problem associated with the space flight or the re-entry trajectory is that of heat protection against the enormous aerodynamic heating. The heating is most intense at the stagnation point of the vehicle. The present paper is discussing gas dynamics in the stagnation region together with the heat conduction in the ablating materials, since the high enthalpy flow is influenced by the conditions at the solid wall and the conditions themselve are dependent on the flow conditions around the body.

A mathematical model of the flow is introduced in the first chapter. The scope of the paper is defined corresponding to the technology of re-entry vehicles. The uniform flow conditions around the body may change with time, since the vehicles travels a great distance in a very short time. By means of simple estimation of characteristic time for transient changes, the problems which should be treated as unsteady are distinguished from those of steady ones. Equations describing state and physical properties in a high enthalpy flow are introduced.

The differential method is introduced as an approximation for the radiation intensity equation. This approximation is applied throughout the present study whenever the radiative effects are involved.

Heat transfer in ablating materials are discussed in the second chapter, since the thermal behavior is dependent upon the properties of materials. We shall investigate graphite, phenolic region separately. An example of deformation of nose cone is calculated for case of sublimating ablation. The optimum shape for the minimum ablation is also discussed.

The mathematical formulation for the gas dynamic flow in the stagnation region is formulated in the third chapter. The fundamental equations together with the boundary conditions are established. The fundamental principle for the solution is also indicated.

The radiation effect in the stagnation point flow is discussed in the last chapter. The results are shown in several figures. Finally the optimum shape for the reduction of the radiative heating is suggested.

Notations

a	pre-exponential factor
A	effective area
B	Boltzmann function
c	velocity of light
c_b	heat capacity
C	condensation, mass fraction
d	parameter
D	diffusion
e	emissibity, internal energy
E	activation energy
E_R	radiation energy density
f	generalized stream function
g	generalized heat function
h	enthalpy
H	total enthalpy
I	specific intensity of radiation
I_X	moment of radiation
J	radiation productivity
k	conductivity
K	heat conductivity
K_n	Knudsen number
l	direction cosine
L	standard length
Le	Lewis-Semenov number
M	Mach number, material constant, molecular weight
p	pressure
p_R	radiative pressure
P_r	Prandtl number
Q	heat
Q_c	heat by conduction
Q_R	heat by radiation
r	radius vector, axial distance
r_b	axial distance of the body
R	gas constant
R_B	radius of curvature of body
R_e	Reynolds number
R_N	radius of curvature of shock wave
t	time
T	Temperature
u	velocity component, similar function
v	velocity of vehicle
U	uniform velocity
v	velocity component
w	mass rate of formation
z	altitude
α	absorption coefficient of radiation
δ	thickness of boundary
Δ	shock standoff distance
ε	pressure ratio on shock wave, $\varepsilon = p/p_s$
ϵ	emissivity
γ	ratio of specific heats, $\gamma = c_p/c_v$
Γ	radiation parameter
λ	mean free path
ρ	density
μ	viscosity, parameter
ν	dynamic viscosity
σ	Stephan-Boltzmann constant
τ	optical length, characteristics time

suffices

b	body
e	boundary layer edge
g	gass
i	i-th species
l	liquid
rad, r	radiation
w	wall

I. Mathematical Formulation of the Problem

1.1 Introduction

At the re-entry envilonment of a shape vehicle or the atmcspheric flight circumstance of a hypwesonic transport plane in the future, the hypervelocity of vehicles introduces complicated phenomena into the flow around the body.

The typical flight conditions for various space vehicles are presumed as indicated in Table 1. [1].

Table 1. Typical Flight Condition

vehicle	altitude	mach number	velocity
hypersonic plane	30 km	15	5 km/sec
manned vehicle	40	30	10
Venus Probe	60	43	13
Mars Probe	60	60	20

It may be reasonable to restrict our study in the following region: altitude is between 20 and 60 km, velocity is between 5 and 20 km/sec. A strong shock wave takes place in front of the blunt nose of the vehicle and the flow field may be divided into three parts: shock wave, shock layer and boundary layer. Gas is suddenly compressed in the shock wave and the kinetic energy of uniform flow transformed into the molecular motion. The thickness of the shock wave is the order of the mean free path λ and the Knudsen number $K_N \equiv \lambda/L \approx M/R_e$ has the order of 10^{-4} when the typical length of the body is 1 m, at a flight condition 10 km/sec at 40 km above sea level. Therefore the shock wave can be considered as a sheet of discontinuity, neglecting the thickness. Yoshikawa[2] calculated the physical conditions behind the shock wave. The temperature and pressure are in the range $6000 \sim 25000°k$, $0.1 \sim 100$ atm respectively corresponding the flight conditions. It is known that the dissociated atoms and ions become strong sorces of radiation.

Invicid shock layer extends between the shock wave and the boundary layer, the pressure, density and temperature remain almost constant when radiation has minor effects. It is characteristic that viscosity and heat conduction are small in this layer. The thickness of the invicid shock layer is practically same as the shock stand off distance, which is calculated from $\Delta/R = \varepsilon/1 + \sqrt{2\varepsilon}$ where R is the radius of curvature at the stagnation point and $\varepsilon = \gamma - 1/\gamma + 1$.[3] Therefore $\Delta/R = 10^{-1}$. The surface of the vehicle is separated by the boundary layer from the invicid shock layer. The radiation energy of hot gas is absorbed and emitted while the heat is transfered by conduction simultaneously. Combustion and/or foreign gas injection into the boundary layer are caused by ablation of the solid wall of the vehicle. Evidently the flow characteristics are largely affected by viscosity in the boundary layer. Since the thickness δ of the boundary layer is about $R/\sqrt{R_e}$, $\delta/R = 3\times10^{-3}$ and $\delta/\Delta = 1\times10^{-2}$ at the designated conditions. Since the composition of gas, temperature and pressure in the boundary layer have a large variety, simple assumptions for state, transport properties may not reflect the real gas effects.

On the surface of the vehicle, application of ablating or sublimating materials is the conventional technology for preventing against the enormous amount of aerodynamic heating. Carrying materials or graphite is extensively used for this purpose. The effects of heat prevention are largely depend upon the physical properties of ablating materials. The principles of heat prevention by these means are followings:

a) The amount of conductive heat is reduced by thickning of the boundary layer due to foreign gas injection introduced by the surface ablation.

b) The large part of heat input to the body is consumed in phase change of the ablating materials and the heat transfer to the body is reduced.
The heat conduction mechanism should be taken in to account for determining the surface conditions.

To sum up, complicated gas dynamic phenomena should be examined in details before coming to the complete understanding of the real situation at the re-entry stage or the atmospheric flight. It does not always impossible to analyse these complicated gas flow even if an electronic computer of extremely capable is available, however it may be equally important to establish a simplified model for understanding the essentials of the phenomena. In the present study, much efforts have been concentrated to the study of hypervelocity gas flow in the region of the stagnation point of a blunt body.

1.2 Fundamental Equations

Equations representing the conservation laws describe the flow field behind the shock wave.

The conservation of mass is given by

$$\frac{\partial \rho}{\partial t} + \mathrm{div}(\rho \boldsymbol{v}) = 0 \tag{1}$$

or $$\frac{\partial \rho}{\partial t} + \rho\, \mathrm{div}\, \boldsymbol{v} + \boldsymbol{v}\, \mathrm{grad}\, \rho = 0$$

The conservation of momentum is expressed as

$$\rho\left[\frac{\partial \boldsymbol{v}}{\partial t} + (\boldsymbol{v}\,\mathrm{grad})\boldsymbol{v}\right] = -\mathrm{grad}\left(p + \frac{4}{3c}\sigma T^4\right) + \mathrm{div}(\mathrm{grad}\,\mu \boldsymbol{v}) + \mathrm{grad}\,\mathrm{div}\left(\zeta + \frac{1}{3}\mu\right)\boldsymbol{v} \tag{2}$$

where the radiation pressure is included for completeness, it is neglegible in the cases of this research. Then the equation is actually the Navier-Stokes equation, where ζ and μ are included in the differential expressions since the viscosity coefficients are strongly depended on temperature.

The energy equation is

$$\rho\left[\frac{\partial h}{\partial t} + (\boldsymbol{v}\,\mathrm{grad})h\right] \tag{3}$$

$$= \frac{\partial p}{\partial t} + (v\ \mathrm{grad})\,p + \mathrm{div}(k\,\mathrm{grad}\,T) + \mu\Phi - \mathrm{div}\,q_R - \mathrm{div}(\rho_i v_i h_i) \quad (3)$$

Finally, the coservation of chemically reacting species can be written

$$\frac{\partial \rho_i}{\partial t} + \mathrm{div}(\rho_i v_i) = \dot{w}_i \quad (4)$$

These equations together with the appropriate boundary conditions furnish the fundamental system of equations for the problem.

The equation of heat conduction in the axial symmetric body yields

$$\mathrm{div}(k\,\mathrm{grad}\,T) = \rho \frac{\partial}{\partial t}(c_b T) \quad (5)$$

where k, ρ, c_b stand conductivity, density and heat capacity, respectively. The coordinate systems are indicated in the figure.

1.3 Boundary Conditions

Boundary conditions expressing the balance of mass and energy on the boundary of the flow field can be obtained in the following way.

(1) Solid Wall

The ablation rate $\dot{m}$ is expressed by

$$\dot{m} = \dot{m}_g + \dot{m}_\ell = (\rho v)_w \quad (6)$$

where $\dot{m}_g$, $\dot{m}_\ell$ mean the mass of gas and liquid per unit time, unit area produced by phase change. The diffusion equation on the wall yields

$$-\left(\rho D \frac{\partial c}{\partial y}\right)_w = (1-c)(\rho v)_w \quad (7)$$

and we have

$$u = 0, \qquad \text{for } y = 0. \quad (8)$$

On the other hand, the heat conducted into solid from the boundary layer $[-Q]_w$ is given by

$$[-Q]_w = \left[k_b \frac{\partial T}{\partial y} - \sum \rho_i v_i h_i - \dot{m} h + \mu u \frac{\partial u}{\partial y} + Q_{rad} \right]_w \quad (9)$$

while the radiation is

$$Q_{rad} = \sigma(\epsilon_g T_g^4 - \epsilon_w T_w^4) \quad (10)$$

where ϵ means the emissivity and suffix g stands for gas. In addition the ablation rate is expressed as a function of wall temperature and pressure, as

$$m = f(T, p). \quad (11)$$

The function is determined by the chemical process of the ablation so that it depends on the properties of ablating materials. For the most cases, the ablation rate is weekly dependent on pressure, so that we have

$$\dot{m} = f(T_w). \quad (12)$$

Therefore the ablation rate or the wall temperature is not determinated from the beginning, but it should be determined by solving equations (9) and (12) simultaneously after finding the states in boundary layer and the solid material.

If combustion or some chemical reaction takes place on the surface, we assume that a heterogeneous reaction

$$2C + O_2 \rightarrow 2CO. \quad (13)$$

Then, the mass production terms are given

$$\left.\begin{aligned} \dot{w}_{co} &= \frac{M_{co}}{M_o} a \rho c e^{-\frac{E}{RT_w}} \\ \text{and} \quad \dot{w}_o &= -\frac{M_o}{M_o} a \rho c e^{-\frac{E}{RT_w}} \end{aligned}\right\} \quad (14)$$

respectively.

(2) Boundary Layer Edge

On the edge of the boundary layer we have relations

$$\left.\begin{aligned} u &= u_e \\ H &= H_e \\ C &= 0 \end{aligned}\right\} \quad (15)$$

for $y = y_e$ or $y \rightarrow \infty$.

(3) Shock Wave

On the shock wave, the Rankine-Hugoniot relation relates the physical quantities behind the shock with those of uniform flow. Therefore the values of physical quantities are known when the shape and the location of the shock is prescribed.

1.4 Differential Approximation for the Equation of Radiative Transfer and Boundary Conditions

The equation of energy flow $I(\Omega)$, in the direction per unit time, unit area, unit solid angle is given by

$$\frac{1}{c}\frac{\partial I}{\partial t} + \mathrm{div}(\Omega I) = a\left(\frac{\sigma}{\pi} T^4 - I\right) \quad (16)$$

for a gray gas in local equilibrium. This is representing the conservation of photons. [5] The heat flux by radiation in the n direction, in other words, the net heat passes through the unit area normal to the n direction per unit time is

$$Q = \Omega \cdot q \quad (17)$$

where

$$q = \int_{4\pi} \Omega I \, d\Omega \tag{18}$$

Therefore, q is a vector function. If we introduce this expression into (3), the energy equation becomes an integro-differential equation, and the solution will be very hard.

We shall apply an approximate solution, which is called "differential approximation". This method was applied by Trangott[6] and Cheng[7] for problems involving the radiation effects.

The moments of specific intensity $I(\tau, \Omega)$ in the Ω direction are obtained by integrating on whole space $\Omega = 4\pi$, after multiplying the direction cosines, thus we have

$$\left.\begin{aligned} I_0 &= \int_0^{4\pi} I \, d\Omega \\ I_{1x_i} &= \int_0^{4\pi} I \, l_i \, d\Omega \\ I_{2x_ix_j} &= \int_0^{4\pi} I \, l_i l_j \, d\Omega \\ &\cdots\cdots \\ I_{nx_ix_j} &= \int_0^{4\pi} I \, l_i l_j^{n-1} \, d\Omega \quad (n \geq 2) \end{aligned}\right\} \tag{19}$$

where l_i stands a direction cosine. Now integrating the equation (5) from 0 to 4π , we have

$$\frac{\partial I_{1x_i}}{\partial x_i} = \alpha I_0 + 4\alpha\sigma T^4 \tag{20}$$

where the unsteady term has been ommitted*. Multiplying l_i^m on the both sides of the equation (16), following system of equation can be obtained successively

$$\frac{\partial I_{2x_ix_j}}{\partial x_j} = -\alpha I_{1x_i}, \quad \frac{\partial I_{3x_ix_i}}{\partial x_j} = -\alpha I_{2x_ix_j}, \text{ etc.} \tag{21}$$

Now let us express I by means of a series of spherical harmonics.

$$I = \sum_{l=0}^{\infty} \sum_{m=-l}^{\infty} (A_{lm}(r)\cos\phi + B_{lm}(r)\sin\phi) \times \left[\frac{2l+1}{4\pi}\frac{(l-m)!}{(l+m)!}\right]^{\frac{1}{2}} P_{lm}(\cos\phi) \tag{22}$$

where

$$\begin{aligned} P_{lm}(x) &= \frac{1}{l!2^l}\frac{d^l}{dx^l}(x^2-1)^l \quad \text{when } m=0 \\ &= (1-x^2)^{m/2}\frac{d^m}{dx^m}P_{l0}(x) \quad \text{when } m\neq 0 \end{aligned} \tag{23}$$

The function I can be expressed approximately by taking finite terms

$$\begin{aligned} I = \frac{1}{\sqrt{4\pi}}A_{00} &+ \sqrt{\frac{3}{2\pi}}\left(-\frac{1}{2}\sin\theta\right)(A_{1-1}\cos\phi \\ &+ B_{1-1}\sin\phi) + \sqrt{\frac{3}{4\pi}}A_{10}\cos\phi \\ &+ \sqrt{\frac{3}{8\pi}}\left(A_{11}\cos\phi + B_{11}\sin\phi\right)\sin\phi \end{aligned} \tag{24}$$

Putting $\Omega = \sin\theta \, d\theta d\phi$, we can calculated the moments

$$\begin{aligned} I_0 &= \frac{1}{\sqrt{4\pi}}A_{00}\int_0^{2\pi}d\phi\int_0^{\pi}\sin\theta\,d\theta = 2\sqrt{\pi}\,A_{00} \\ I_1 &= 2\pi\sqrt{\frac{3}{4\pi}}A_{10}\int_0^{\pi}\cos^2\theta\sin\theta\,d\theta = \sqrt{\frac{4\pi}{3}}A_{10} = Q \\ I_2 &= \frac{4\pi}{3}A_{10} \\ I_3 &= -\frac{4\pi}{3}B_{11} \end{aligned} \tag{25}$$

Finally, we have

$$\begin{aligned} &\text{div grad } I_0 - \text{grad } I_0 \frac{1}{\alpha}\text{grad}\,\alpha - 3\alpha^2(I_0 - 4\pi B) = 0 \\ &q = -\frac{1}{3\alpha}\text{grad } I_0 \\ &\text{div } q = -\alpha(I_0 - 4\pi B) \end{aligned} \tag{26}$$

where $B = \sigma/\pi T^4$. Thus the energy equation can be expressec in a form of a differential equation when the relation (26) is introduced in (3). The boundary conditions for radiation can be obtained in the similar way.

On the shock wave, we have

$$\frac{1}{4}I_0 - \frac{1}{2}Q_2 = \epsilon_\infty \sigma T^4 \tag{27}$$

where Q_2 is the radiative energy passing through the shock wave normally from in the direction of the main flow, when the shock is transparent.

On the surface of the body, we have

$$\frac{1}{4}I_0 + \frac{1}{2}Q_2 = \epsilon_w \alpha_w T_w^4 \tag{28}$$

where Q_2 is the heat flux directed to the boundary layer when the surface of the body is transparent for radiation.

1.5 Real Gas Effect at the Extremely High Temperature

At the extremely high temperature, one can not expect that the equation of state for perfect gas holds for a real gas. The equilibrium state behind a strong shock wave should be investigated means of kinetic theory of gas. However, equations

$$\left.\begin{aligned} \rho h &= a p^l \\ T &= A p^m h^n \end{aligned}\right\} \tag{29}$$

and

together with the thermodynamic relation

$$\left[\frac{\partial e}{\partial(1/\rho)}\right]_T = T\left(\frac{\partial p}{\partial T}\right)_\rho - p \tag{30}$$

and

$$e = h - p/\rho$$

are assumed and the constants involved in these equations are determined from the experimental data [8] by means of the method of least squares.

Thus, we have

$$\left.\begin{aligned} \rho h &= 6.02\ p \\ T &= 1.213\ p^{0.072}\ h^{0.555} \end{aligned}\right\} \tag{31}$$

(C.G.S.)

* See 1.7

in the range

$$0.1 < p < 10 \text{ atm}, \quad 2000\ k^{\circ} < T < 23000^{\circ}k.$$

We also determined the absorption coefficient α and the viscosity η in the same way, yielding

$$\left.\begin{aligned} \alpha &= 1.702 \times 10^{-37}\ p^{1.604}\ h^{2.03} \\ \text{and} \quad \eta &= 1.597 \times 10^{-7}\ h^{0.346} \end{aligned}\right\} \tag{32}$$

1.6 Transport Properties

For the exact analytical treatment of the boundary layer of mixed gas, we have to express the transport properties in terms of those of component gases. Hirschferder et. al,[9] and Bird et. al.[10] obtained these expressions on the basis of kinetic theory of gas. The complicated expressions will not be reproduced in this paper, in short, the transport properties of the mixed gas can be expressed by molecular weight, concentration and thermodynamical properties of component gases.

1.7 Quasi-Steady Analysis

Re-entry vehicles approach to the surface of the earth at a hypersonic speed. Atmospheric states, density pressure and temperature as well as the velocity of the vehicle change a great deal in a very short time. Therefore, we have to take the change of environment into account of the investigation of re-entry aerodynamics. On the other hand, according to an intense heat input at the surface of the body, the temperature of the body will be raised gradually so that the ablation rate will be increased in the course of re-entry trajectory. Moreover, the surface of the vehicle may recess according to the ablation rate. Therefore, every phenomenon depends on time and one must study the unsteady case instead of the steady one. Obviously to include a nonsteady term in each equation will increase the difficulty of the problem. It will be advisable to investigate the possibility of quasi-steady analysis before we take up the study of solutions.

The equation of motion of a no-lifting vehicle is given by

$$C_D \frac{1}{2} \rho V^2 S = \alpha W \tag{33}$$

when α denotes the maximum allowable acceleration. The atmospheric density ρ is expressed in terms of the altitude from the sea level as

$$\rho = \rho_0 e^{-hz} \tag{34}$$

where $h = 0.141 \times 10^{-3}\ m^{-1}$, $\rho_0 = 0.125$ kg sec^2/m^4.

Since we have

$$V = -\frac{dz}{dt} \tag{35}$$

the time rate of change of the atmospheric density is given as

$$\frac{d\rho}{dt} = hV\rho \tag{36}$$

Therefore the characteristic time for the density change during the re-entry flight is

$$\tau_\rho = 1/hV \tag{37}$$

Under the circumstances of interesting, $\tau_\rho \approx 1$. Since this is the case of vertical flight at non lifting condition, the characteristic time for the trajectory of lifting vehicle will be much less than this value. From the equation of state of the air, we know that the characteristic times for the change of atmospheric pressure and temperature are the same order of density change.

Now, let us examine the characteristic time of physical quantities in the boundary layer of thickness δ subjected to the sudden change of conditions at the edge or the wall. The change would diffuse in the course of time throughout the boundary layer. The characteristic time for this diffusive process might be estimated by one-dimensional theory: the basic equation is given

$$\frac{\partial u}{\partial t} = \nu \frac{\partial^2 u}{\partial y^2} \tag{38}$$

and the characteristic time is

$$\tau_u = \delta^2/\nu \tag{39}$$

This is the result of a simple incompressible analysis, however the order of the characteristic time would not essentially different even for the compressible boundary layer in a hypersonic flow. Now in the stagnation point region, where $u_e = ax$, $\delta \propto \sqrt{\nu/a}$ hence we have

$$\tau_u = 1/a \tag{40}$$

At the condition of the interesting environment a is the order of 10^4 sec^{-1}, therefore τ_u is neglesible in comparison of τ_ρ.

The characteristic time for the temperature change in the boundary layer can be estimated by the formula

$$\tau_T = P_r \tau_u \tag{41}$$

Since the Prandtl number is the order of unity, the characteristic time is the same order as that of velocity change.

On the other hand, the characteristic time for the radiation is the order of Δ/c, since the radiative energy is transfered by means of a magnetic wave. Thus we have $\tau_R = 0(10^{-9})$.

From the one dimensional heat conduction equation in a solid material, the characteristic time τ_T for the heat conduction is L^2/c^2 where L, c^2 are the typical length and the thermal diffusibility of the material, respectively. For example, $c^2 = 10^{-4} m^2/sec$ for graphite, therefore τ_c has the order of 10^2sec. when L is the order of 10^{-1}m.

It will be shown that the characteristic time

for the change of the surface temperature is the order of 1 sec. for ablating materials.

Summarizing, the characteristic time for the change of physical quantities during the re-entry trajectory are indicated in Table 2.

Table 2. Characteristic Times

change in	characteristic time
atmospheric environment	1
boundary layer	10^{-4}
heat transfer in solid	1
radiative transfer	10^{-9}

Therefore, boundary layer and the radiative transfer can be treated to be in a quasi-steady state while for the ablation process and the uniform flow conditions, the unsteady change should be taken into account of the analysis.

II Unsteady Heat Transfer in Ablating Materials

2.1 Graphite

Graphite is applied extensively as an ablator for a space vehicle. Diaconis et. al.[11], Scala [12] studied the thermodynamical performances of this material. However few studies have been conducted for undteady cases. Recently Nomula [13] investigated theoretically the unsteady heating of graphite and obtained a satisfactory coincidence with the experiments.

In the present study, to establish a simple theory of unsteady ablation, a model of thermodynamical properties of graphite is introduced and the one dimensional heat conduction is solved to obtain the surface temperature as well as the temperature distribution in the body.

(1) Mathematical Formulation of the Problem

In the stagnation point region, we can assume that

$$\frac{\partial T}{\partial x} \ll \frac{\partial T}{\partial y}, \quad \frac{\partial^2 T}{\partial x^2} \ll \frac{\partial^2 T}{\partial y^2} \tag{1}$$

then the heat conduction equation reduces to the one dimensioned equation

$$\frac{\partial}{\partial y}\left(k \frac{\partial T}{\partial y}\right) = \rho \frac{\partial}{\partial t}(C_b T) \tag{2}$$

where y is directed to the inside of the body from the surface. k, ρ, C_b depend upon the temperature T. We can put

$$\left.\begin{aligned} k(T) &= k\, T^{-n}, \quad n = 0.077 \\ C_b(T) &= C_{bo}\, T^{m}; \quad m = 0.137 \\ \rho(T) &= \rho_o \end{aligned}\right\} \tag{3}$$

k_o = 0.33 cal/cm. sec. deg C_{bo} = 0.17 cal/g deg ρ_o = 1.55 gr/cm. This model (thick lines) is compared with the real thermodynamical properties (dotted lines) in Fig 1.

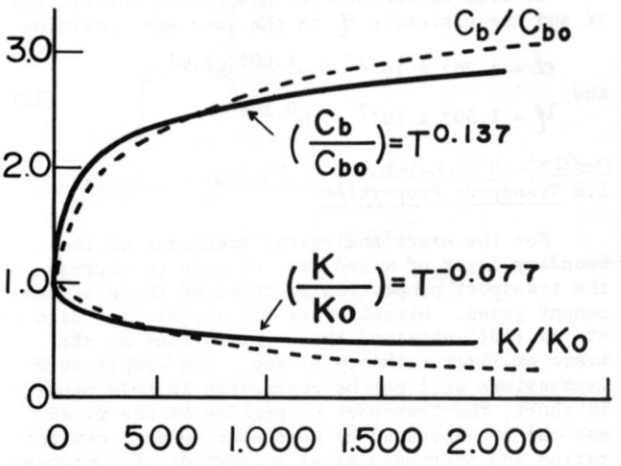

FIGURE 1 Properties of Graphite

Now, the equation turns out

$$k_o \frac{\partial}{\partial y}\left(T^{-n}\frac{\partial T}{\partial y}\right) = (m+1)\rho_o C_{bo} T^{m} \frac{\partial T}{\partial t} \tag{4}$$

where

$$K \equiv (m+1)\frac{\rho C_{bo}}{k_o} = 0.91 \quad \text{sec/cm}^2 \tag{5}$$

The equation can be rewritten as

$$T\frac{\partial^2 T}{\partial y^2} - n\left(\frac{\partial T}{\partial y}\right)^2 = K T^{\gamma}\frac{\partial T}{\partial t} \tag{6}$$

where $\gamma = m + n + 1 = 1.214$.

(2) Similar Solutions

If we put

$$T = t^{\frac{1-2\mu}{\gamma-1}}\, u(\zeta), \quad \zeta = \frac{y}{t^{\mu}} \tag{7}$$

then equation (6) yields

$$t^{2\frac{1-2\mu}{\gamma-1}-2\mu} u u'' - n t^{2\frac{1-2\mu}{\gamma-1}-2\mu} u'^2 = K t^{\gamma\frac{1-2\mu}{\gamma-1}+\frac{1-2\mu}{\gamma-1}-1}\left[\frac{1-2\mu}{\gamma-1}u - \zeta\mu u'\right]u^{\gamma}$$

Since we have

$$\gamma\frac{1-2\mu}{\gamma-1} + \frac{1-2\mu}{\gamma-1} - 1 = 2\frac{1-2\mu}{\gamma-1} - 2\mu,$$

the factors involving t drop out from both sides of the equation and finally yielding an equation for u

$$uu'' - nu'^2 = K\left[\frac{1-2\mu}{\gamma-1}u - \mu\zeta u'\right]u^{\gamma} \tag{8}$$

(3) Initial and Boundary Conditions

The conventional initial and boundary conditions for one dimensional heat conduction are

$T(y, 0) = f(y)$: initial temperature distribution

$$T(\infty, t) < \infty$$

$$\left[k \frac{\partial T}{\partial y} \right]_{y=0} = -d : \text{heat input at the surface } y=0. \tag{9}$$

The last relation can be rewritten as

$$k_0 \left(\frac{\partial T}{\partial y} \right)_0 = -d(T_0)^n \tag{10}$$

Hence, we have for $u(y,t)$

$$\left.\begin{aligned} & k_0 \left(\frac{\partial u}{\partial y} \right)_0 = -d u^n(0,t) \\ & u(\infty) = 1 \end{aligned}\right\} \tag{11}$$

and

$$k_0 t^{\frac{1-2\mu}{\gamma-1}-\mu} u'(0) = -dt^{\frac{1-2\mu}{\gamma-1}} u^n(0)$$

Since this equation should hold independent of t,

$$\frac{1-2\mu}{\gamma-1} - \mu = \frac{1-2\mu}{\gamma-1}$$

must hold, hence we have

$$\mu = \frac{1-n}{2+m-n} = 0.45 \tag{12}$$

and

$$\frac{1-2\mu}{\gamma-1} = 0.49 \tag{13}$$

Therefore we have

$$u'(0) = -\frac{d}{k_0} u^n(0) \tag{14}$$

and

$$T = t^{0.49} u(\zeta) \tag{15}$$

A solution for $u(\zeta)$ is shown in Fig 2. The variation of the surface temperature are indicated in Fig 3 and compared with the experiments conducted by Nomura.[13] The surface temperature is always given by

$$T_w(t) = A\, t^{0.49} \tag{16}$$

where the constant $A \equiv u(0)$ are determined by the heat input Q. The coefficient A in the equation (16) can be determined in terms of the heat input Q or d.

When combustion or the radiation at the surface are involved, since the heat input on the surface is a function of the surface temperature, the similar solution does not exist for the problem. However, the heat input is determined neglecting the unsteady change, the surface temperature would be determined by trial and error method, modifying the heat input d in (9) or A in (16).

However, if the heat input at the stagnation point changes slowly with time in the course of the re-entry trajectory. The transient heat conduction should be investigated for the case when d is a function of time. Considerable numerical computations will be required before we solve this problem completely. However if the thickness of graphite is finite and the temperature is raised to 1000°C, then the thermodynamical properties can be considered as constant, as is observed in Fig 1. Then the one dimensional heat conduction problem will be solved without difficulty.

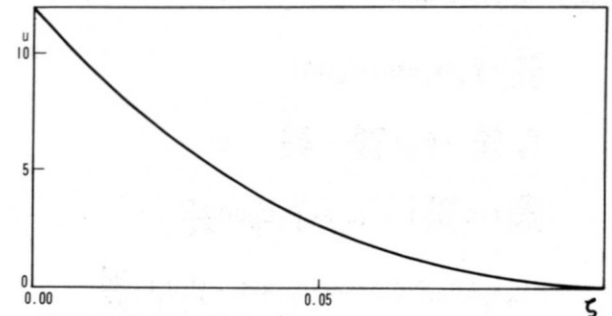

FIGURE 2 The Similar Solution $u(\zeta)$

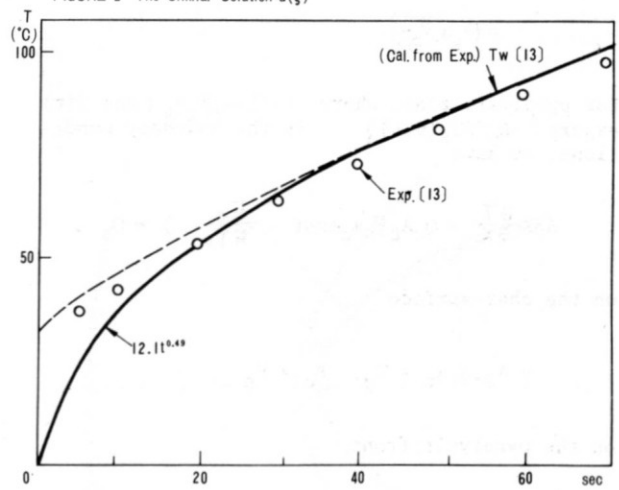

FIGURE 3. Surface Temperature

2.2 Plastics

Plastics, such as phenolic resin, epoxy resin involves a pyrolysis reaction under the ablating conditions. Swann et.al.[14] considered that the reaction is confined in a sheet when they studied the unsteady ablation of charring materials. We presumed that pyrolysis reaction takes place in a finite zone and the produced gas is injected through capillary holes in char and pyrolysis zones to the boundary layer.[15] Moreover, we assumed that the pyrolysis rate is given

$$\dot{m} = A \rho a_p \exp(-E_p/RT) \tag{17}$$

and the char removal is dominated by the heterogeneous oxidation as

$$\dot{m}_c = A \rho a_c \exp(-E_c/RT) \tag{18}$$

where A stands for the effective solid area in a

constant cross sectional area.

The equations are

$$\frac{\partial}{\partial x}\,[\,F\,] = 0 \tag{19}$$

and

$$\frac{\partial}{\partial x}(A_0 K \frac{\partial T}{\partial x}) - (C_p F + \rho C_p A_0 U)\frac{\partial T}{\partial x} = A_0 \rho_s C_p \frac{\partial T}{\partial t} \tag{20}$$

for char layer and

$$\frac{\partial F}{\partial C} = \rho_s A a_p \exp(-E_p/RT)$$

$$\rho_s \frac{\partial A}{\partial t} + \rho_s U \frac{\partial A}{\partial x} + \frac{\partial F}{\partial x} = 0$$

$$\frac{\partial}{\partial x}(AK\frac{\partial T}{\partial x}) - (C_p F + \rho_s C_p A U)\frac{\partial T}{\partial x}$$

$$-\rho_s a_p A(C_p T - Q_r)\exp(-E_p/RT) - \rho_s C_p U T \frac{\partial A}{\partial x}$$

$$= \rho_s a_p \frac{\partial TA}{\partial x}$$

for pyrolysis zone, where $F=(1-A)\rho_g V_g$ and $U(t) = a_c \exp\{-E_c/RT_s(0,t)\}$. As the boundary conditions, we have

$$A_0 K \frac{\partial T}{\partial x} = Q_c A_0 \rho_s a_c \exp\left(-\frac{E_c}{RTs}\right) + Q_s$$

on the char surface

$$A = A_0, \quad A_c = T_p, \quad F_c = F_p$$

on the pyrolysis front

$$T = T_{-\infty}, \quad F = 0, \quad A = 1.0$$

in the virgin material.

The fundamental equations are solved numerically with boundary conditions. Fig 4 is indicating a typical results where the surface temperature are shown as a function of time. The results are compared with experiments.

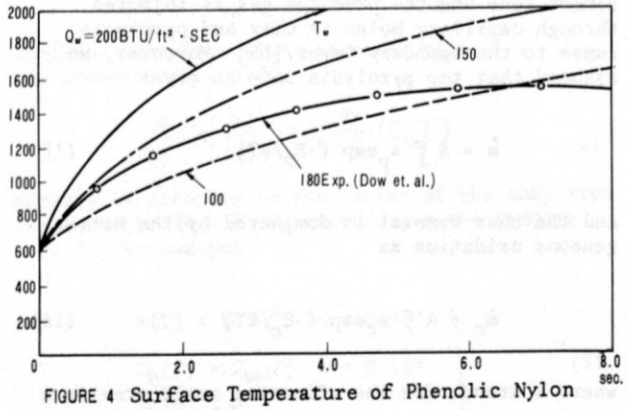

FIGURE 4 Surface Temperature of Phenolic Nylon

2.3 Deformation of Conical Nose by Sublimating Ablation

The deformation of re-entry body in a hypersonic flow is a problem of interesting for space technology. The process of determining the ablation rate is indicated on Fig 5.

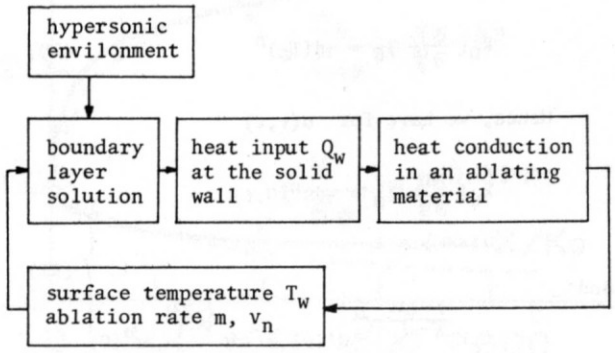

FIGURE 5 Process of Determining the Ablation Rate.

The boundary layer and the heat conduction in the ablating material should be solved simultaneously. Trial and error method can be applied to determine the wall temperature as well as the ablation rate. However, if the surface temperature is prescribed, and the heat transfered into the solid can be neglected, then we can put the heat input is proportional to the ablation rate. Kondo[16] calculated the deformation of the blund body. Fig 6 is representing the deformation of a conical nose of vertex angle 60°. The deformation rate is given as

$$V_w = E\,\xi^{-\frac{1}{4}}\{3.569 - (48.43+12.99D^{\frac{2}{7}})\xi + (257.4-28.84D^{\frac{2}{7}})\xi^2 - (2233+100.8D^{\frac{2}{7}})\xi^3\} \tag{22}$$

when the profile of the cone is expressed as

$$r_b/R = \xi - 5.208\xi^2 + 24.31\xi^3 - 52.08\xi^4 + 41.67\xi^5$$

where $\xi = x/R$, $E = \dfrac{\gamma^2 R \rho_\infty \mu_b M^2 U}{\sqrt{2}(\gamma+1) He\, g_b \rho_w}$

and $D = \dfrac{2\gamma^2 M^2 \mu_b R^3 U}{7(\gamma-1)\, He\, g_b}$ (23)

Newtonian approximate formula has been applied to find the velocity distribution on the edge of the boundary layer.

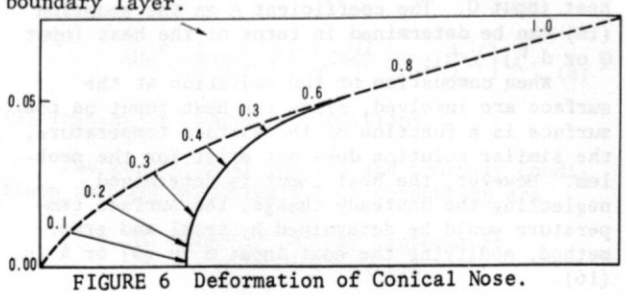

FIGURE 6 Deformation of Conical Nose.

2.4 Optimum Shape

To find an optimum shape to reduce the amount of ablation in the stagnation region is a problem of interesting. When the ablation rate is determined as a functional of the body shape $r_b(\xi)$ by means of the process designated in Fig 6, then, the problem will be expressed in the framework of variational principle

$$\int_0^L \dot{m}(\xi) 2\pi r_b(\xi) \sqrt{1+r_b'^2}\, d\xi \ : \text{Min.} \tag{24}$$

where $\dot{m} = F[r_b(\xi)]$.

If we simply assume that $\dot{m} \propto Q_w$, T_w = const. and [17]

$$Q_w = \frac{0.763 P_r^{-0.6}}{\sqrt{\rho_\infty u_\infty \xi / \mu_\infty}} \rho_\infty u_\infty C_p (T_w - T_{aw}) \tag{25}$$

then (24) turns out to be

$$\int_0^L A \xi^{-\frac{1}{2}} [1+r_b'^2]\, d\xi \ : \text{Min.} \tag{26}$$

Euler's condition will be integrated to give optimum shape

III Fundamental Equations of Stagnation Flow

3.1 Assumptions

The present analysis is based on the following assumptions:

1) The surface temperature of a sublimating material is constant and independent of the sublimating rate.

2) The gas mixture behabes as a perfect gas, consequently the equation of state

$$p = \rho \bar{R} T, \quad (\bar{R} = \Sigma C_i R_i) \tag{1}$$

holds.

3) There is no chemical reaction on the surface of the body nor in the flow region.

4) The boundary layer assumptions hold at the stagnation point, even if there exists a gas injection due to sublimation.

5) Thermal diffusion and pressure diffusion are negligible.

6) The Lewis-Semenov number is constant and assumed equal to 1.

$$Le = \bar{C}_p D_{12} \rho / k = 1 \tag{2}$$

7) The Prandtl number of the mixed gas is constant and assumed equal to 0.7.

$$P_r \equiv \bar{C}_p \mu / k = 0.7, \quad (\bar{C}_p = \Sigma C_i C_{pi}) \tag{3}$$

8) A linear viscosity-temperature law holds, so that

$$\frac{\mu}{\mu_b} = \frac{T}{T_b} \quad \text{or} \quad \frac{\mu \rho}{\mu_b \rho_b} \equiv N = 1 \tag{4}$$

9) The injection rate is proportional to the heat transfer $-q_w$ from the boundary layer to the body, so that we have

$$-q_w = M v_w \tag{5}$$

where M depends upon the properties of the sublimating materials.

10) The flow is laminar and steady.

3.2 Fundamental Equations

The fundamental equations 1.2(1) $\sim$ (4) yield for the present problem: The overall continuity equation for the gas mixture is

$$\frac{\partial \rho u r}{\partial x} + \frac{\partial \rho v r}{\partial y} = 0 \tag{6}$$

where the coordinate x is measured along the body surface from the nose, the coordinate y is measured along the ourward normal from the body surface, r is the cylindrical radius from the axis of symmetry to any point in the boundary layer, u and v are the velocity components in the x and y directions, respectively. Since we have assumed that the boundary layer thickness is small in comparison with the radius of the body cross section so that for an axial symmetric flow we may replace $r(x)$ by $r_b(x)$.

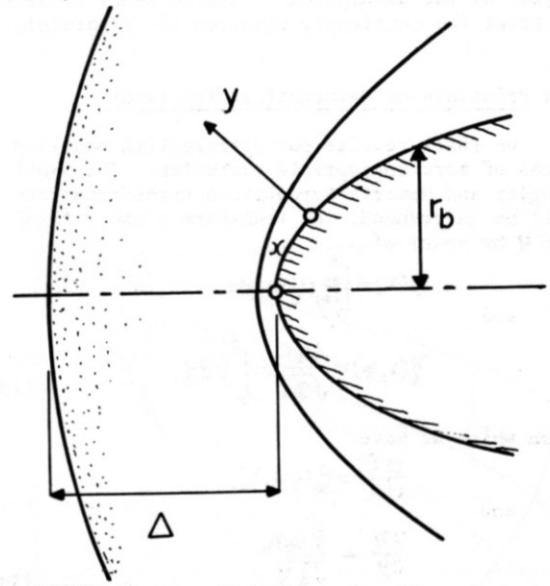

FIGURE 7 Flow Field Around a Blunt Body

The continuity equations fo each species are

$$\rho u \frac{\partial C_i}{\partial x} + \rho v \frac{\partial C_i}{\partial y} = \frac{\partial}{\partial y}\left(\rho D_{12} \frac{\partial C_i}{\partial y}\right) + w_i \tag{7}$$

where C_i is the mass fraction of the i-th component (with $\Sigma C_i = 1$), w_i the mass rate of formation of the species per unit volume per unit time, and D_{12} the binary diffusion coefficient. In order that the mass be conserved in any chemical change we require $\Sigma w_i = 0$.

The momentum equation is given

$$\rho u \frac{\partial u}{\partial x} + \rho v \frac{\partial u}{\partial y} = -\frac{\partial p}{\partial y} + \frac{\partial}{\partial y}\left(\mu \frac{\partial u}{\partial y}\right) \tag{8}$$

$$\rho u\frac{\partial H}{\partial x}+\rho v\frac{\partial H}{\partial y}=\frac{\partial}{\partial y}\left(\frac{\mu}{P_r}\frac{\partial H}{\partial y}\right)+\frac{\partial}{\partial y}\left[\mu\left(1-\frac{1}{P_r}\right)\frac{\partial}{\partial y}\left(\frac{u^2}{2}\right)\right]$$
$$+\frac{\partial}{\partial y}\left[\rho D_{12}\left(1-\frac{1}{Le}\right)\sum\left(h_i-h_i^\circ\right)\frac{\partial C_i}{\partial y}\right] \tag{9}$$

where

$$H=h+\frac{1}{2}u^2=\sum C_i\left(h_i-h_i^\circ\right)+\frac{1}{2}u^2, \tag{10}$$

and h_i° is the heat liberated in the formation of the i-th component at 0°K.

3.3 Boundary Conditions

The boundary conditions are

$$\text{at } y=0;\ u=0,\ v=v_b,\ H=H_b,\ C_i=C_{ib}, \tag{11}$$

and

$$\text{at } y\to\infty;\ u\to u_e,\ H\to H_e,\ C_i\to C_{ie}, \tag{12}$$

where we have assumed that the temperature at the surface near the stagnation point is constant and is independent of the ablating rate or the heat transfer rate. The subscripts b and e denote the conditions at the body surface and at the edge of the boundary layer, respectively.

The last term of the equation (9) will disappear by the assumption 6) and we shall be able to treat the continuity equation (7) separately.

3.4 Principle of Mathematical Treatment

We shall rewrite our differential equation in terms of more appropriate variables. The usual Mangler and Howarth-Dorodnitsyn transformations will be introduced. We transform x and y to ξ and η by means of

$$\xi(x)=\int_0^x \rho_b\mu_b u_e r_b^2\,dx,$$

and

$$\eta(x,y)=\frac{u_e r_b}{\sqrt{2\xi}}\int_0^y \rho\,dy, \tag{13}$$

from which we have

$$\frac{d\xi}{dx}=\rho_b\mu_b u_e r_b^2,$$

and

$$\frac{\partial\eta}{\partial y}=\frac{\rho u_e r_b}{\sqrt{2\xi}} \tag{14}$$

We also define as the dependent variables the following dimensionless quantities:

$$f=\int_0^\eta \frac{u}{u_e}\,d\eta, \tag{15}$$

and

$$g=\frac{H}{H_e}. \tag{16}$$

The continuity equation (6) is integrated with respect to y and we have after some manipulations,

$$(\rho v-\rho_b v_b)r_b=-\frac{\partial}{\partial x}\int_0^y \rho u r_b\,dy$$
$$=-\left[\frac{d\xi}{dx}\frac{\partial\sqrt{2\xi}f}{\partial\xi}+\sqrt{2\xi}\frac{\partial\eta}{\partial x}\frac{\partial f}{\partial\eta}\right] \tag{17}$$

We obtain for the momentum equation, the relation

$$\frac{\partial^3 f}{\partial\eta^3}+f\frac{\partial^2 f}{\partial\eta^2}+2\frac{d\ln u_e}{d\ln\xi}\left[\frac{\rho_e}{\rho}-\left(\frac{\partial f}{\partial\eta}\right)^2\right]-\frac{\sqrt{2\xi}\,v_b}{\mu_b u_e r_b}\frac{\partial^2 f}{\partial\eta^2}$$
$$=2\xi\left(\frac{\partial f}{\partial\eta}\frac{\partial^2 f}{\partial\eta\partial\xi}-\frac{\partial f}{\partial\xi}\frac{\partial^2 f}{\partial\eta^2}\right) \tag{18}$$

while we have for the energy equation

$$\frac{\partial^2 g}{\partial\eta^2}+P_r f\frac{\partial g}{\partial\eta}+(P_r-1)\frac{u_e^2}{H_e}\left\{\frac{\partial f}{\partial\eta}\frac{\partial^3 f}{\partial\eta^3}+\left(\frac{\partial^2 f}{\partial\eta^2}\right)^2\right\}$$
$$-P_r\frac{\sqrt{2\xi}\,v_b}{\mu_b u_e r_b}\frac{\partial g}{\partial\eta}=2\xi P_r\left(\frac{\partial f}{\partial\eta}\frac{\partial g}{\partial\xi}-\frac{\partial f}{\partial\xi}\frac{\partial g}{\partial\eta}\right) \tag{19}$$

The boundary conditions may be written as follows:

$$\text{at } \eta=0;\ f(0)=0,\ \frac{\partial f}{\partial\eta}=0, \tag{20}$$
$$g(0)=g_b\ (=\text{const.})$$

and

$$\text{at } \eta\to\infty;\ \frac{\partial f}{\partial\eta}\to 1,\ g\to 1, \tag{21}$$

The overall continuity relation is not required since it is automatically satisfied by the transformed variables.

The continuity equation (7) for each species turns out

$$\frac{\partial^2 C_i}{\partial\eta^2}+P_r f\frac{\partial C_i}{\partial\eta}+2P_r\frac{\xi}{\rho u_e}\frac{dx}{d\xi}w_i-P_r\frac{\sqrt{2\xi}\,v_b x_i}{\mu_b u_e r_b}$$
$$=2\xi P_r\left(\frac{\partial f}{\partial\eta}\frac{\partial C_i}{\partial\xi}-\frac{\partial f}{\partial\xi}\frac{\partial C_i}{\partial\eta}\right) \tag{22}$$

and the boundary conditions are

$$\text{at } \eta=0;\ C_i(0)=C_{ib}\ (=\text{const.}) \tag{23}$$

and

$$\text{at } \eta\to\infty;\ C_i(\eta)\to C_{ie}\ (=0 \text{ or } 2) \tag{24}$$

corresponding to (11) and (12).

3.5 Stagnation Point Solutions

Near a stagnation point of a blunt-nosed body, we can assume the existence of a similar solution. In other words, f, g and C_i can be regarded as the functions of η alone. Furthermore, u_e^2/H_e is negligibly small, so the boundary layer equations (18) and (19) reduce to

$$f'''+(f-v_0)f''+\frac{1}{2}(g-f'^2)=0 \tag{25}$$

and

$$g''+P_r(f-v_0)g'=0 \tag{26}$$

where the prime denote the differentiation with respect to η. The coefficient 1/2 in the momentum equation is obtained from the conditions that in the region near the stagnation point $r_b=x$ and $u_e=x\left(\frac{du_e}{dx}\right)_0$, so that from (14), $\xi\propto x^4$ as $x\to 0$. We put $\rho_e/\rho=g$ for a perfect gas with constant specific heats. We define the nondimensional injection

$$v_0 = \sqrt{\frac{\rho_b}{2\mu_b}}\ \frac{v_b}{\sqrt{\left(\frac{du_e}{dx}\right)_0}} \tag{27}$$

The boundary conditions (20) and (21) are written as

$$\text{at } \eta = 0;\ f(0) = f'(0) = 0,\ g(0) = g_b \tag{28}$$

and

$$\text{at } \eta = \infty;\ f'(\eta) \to 1,\ g(\eta) \to 1. \tag{29}$$

Kondo et. al.[17] have obtained the solutions on a digital computer for several values of v_0 and g_b.

We note that for a perfect gas and enthalpy a function of temperature alone, the heat transfer rate at the surface of a body may be expressed as

$$-\dot{q}_b = \left(\frac{k}{c_p}\frac{\partial h}{\partial y}\right)_w = \frac{k_b H_e}{c_{pb}}\left(\frac{u_e \rho_b r_b}{\sqrt{2\xi}}\right) g'(0)$$

$$= \frac{\sqrt{2}\, H_e k_b}{c_{pb}}\left[\frac{\rho_b}{\mu_b}\left(\frac{du_e}{dx}\right)_0\right]^{\frac{1}{2}} g'(0) \tag{30}$$

We assume that the injection rate is proportional to the heat transfer rate $-\dot{q}_b$, consequently from (28) and (31), we have

$$\frac{\sqrt{2}\, H_e k_b}{c_{pb}}\left[\frac{\rho_b}{\rho}\left(\frac{du_e}{dx}\right)_0\right]^{\frac{1}{2}} g'(0) = M\sqrt{\frac{2\mu_b}{\rho_b}\left(\frac{du_e}{dx}\right)_0}\, v_0 \tag{31}$$

or

$$g'(0) = K v_0$$

where

$$K = \frac{P_r}{H_e \rho_b} M \tag{32}$$

Because the sublimating temperature and the coefficient sublimating rate M depend on the sublimating substance, and K can be considered as a constant when the flow condition H is prescribed.

From the assumption of no chemical reactions, we can set $\dot{w}_i = 0$, therefore we have

$$C_i'' + P\,(f - v_0) C_i' = 0 \tag{33}$$

and the boundary conditions reduce to

$$\text{at } \eta = 0;\ C_i(0) = C_{ib} \tag{34}$$

and

$$\text{at } \eta \to \infty\ ;\ C_i(\eta) \to C_{ie} \tag{35}$$

We note that (26) is the same equation as (33). Hence C_i and g must be connected by the relation

$$C_i = C_{ib} + \frac{g - g_b}{1 - g_b}\,(C_{ie} - C_{ib}). \tag{36}$$

IV Radiation in Stagnation Point Flow

4.1 Stagnation Point Flow

Let us restrict our investigation in the stagnation point region and neglect the effects of viscosity. Physical quantities u, v, p, h, ρ, I_0, T, η and α are expanded in power series, for example

$$u(r, \theta) = \sin\,[u_1(r) + u(r)\sin^2\theta + u_3(r)\sin^4\theta + \cdots] \tag{1}$$

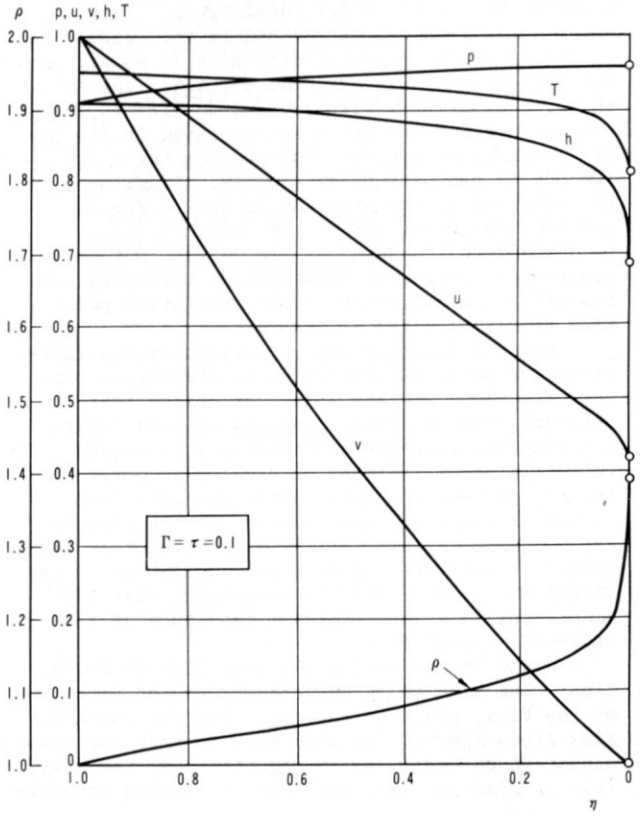

FIGURE. 8a Distribution of Physical Quantities

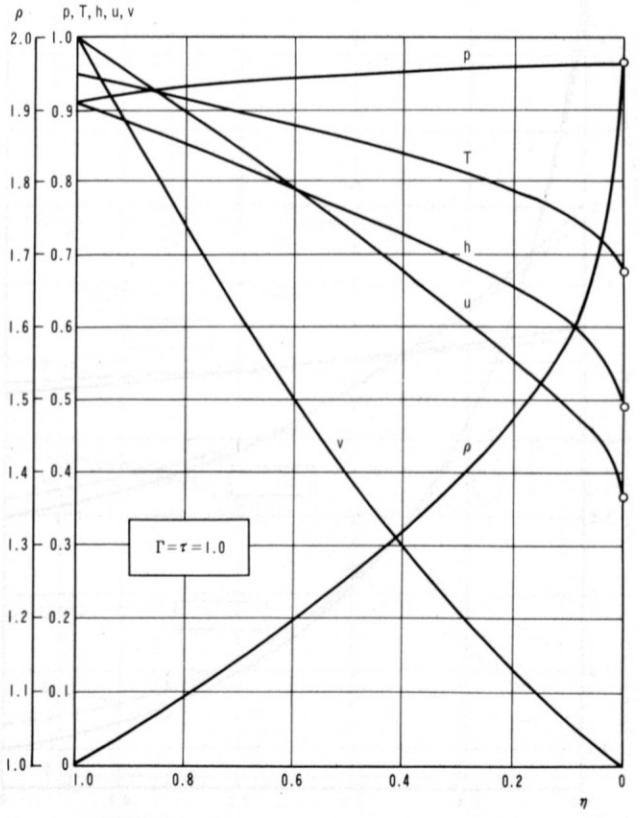

FIGURE. 8b Distribution of Physical Quantities

where γ , θ are the polar coordinates. Then, these quantities are introduced in the fundamental equations and a system of differential equations for the coefficients are deduced, after comparing the same order term with respect to $\sin\theta$. The boundary conditions are also expressed in the polar coordinates system. The problem turns out two points boundary value problem. Starting from the shock wave, the solution is looked for to satisfy the conditions on the wall.

Numerical computaions are carried out on an electronic computer. Some typical solutions for the effect of radiation in the stagnation point flow are illustrated in figures.

Fig 8 indicating the variations of the representative physical quantities in the region between the shock and the body. We notice that the pressure remains almost constant in this region. Considerable decrease of enthalpy is observed while the steep increase of density is noted in the region near the body. When the radiation effect is stronger, the enthalpy of the flow decreases more rapidly. It is also noted that the normal velocity decreases almost uniformly to the stagnation point. This is suggesting that the simple analysis is useful for the study of the stagnation point flow.

Fig 9 is indicating the heat flux of radiation. The sign of q_R corresponds to the direction of the flux, positive q_R means that the radiation flux flows against the main flow through the transparent shock wave. q_R is negative near the body, this is denoting that the heat is flowing into the surface of the body. The amount of heat, reflected or absorbed is increased with the radiation parameter Γ.

Fig 10 is showing the normal velocity along the stagnation streamline behind the shock together with the pressure distributions for various Γ. The abscissa of the figure denotes the normalized distance from the shock where the radius of the shock is taken as the standard. Since the points for v=0 correspond to the surface of the body. We can find the shock standoff distance, which is also indicated in Fig 12 in terms of Γ .

Fig 11 describes the change of tangential velocity since the effect of viscosity has not been included in the present analysis, the velocity does not vanish at the wall. We notice that the velocity is decreasing almost uniformly after the shock wave.

Fig 12 is indicating the influence of and on the shock standoff distance Δ . When the effect of radiation becomes stronger, the density is increased. This will be noticed when Fig 8a and Fig 8b. Therefore the shock approaches to the body when the effect of radiation is included. The shock standoff distance in a hypersonic flow is estimated by $\Delta = \varepsilon/1+\sqrt{2\varepsilon}$ when radiation is not involved in the flow or $\Gamma \to 0$. The optical thickness has a minor effect on the shock standoff distance. Large optical thickness means that the mean free path of the photon is small or the collision frequency with the gas particles are large so that the radiative energy is sufficiently absorbed by gas. This fact will explain the differences of the curves in Fig 9 and Fig 12. The effect of the optical thickness on the enthalpy distribution is

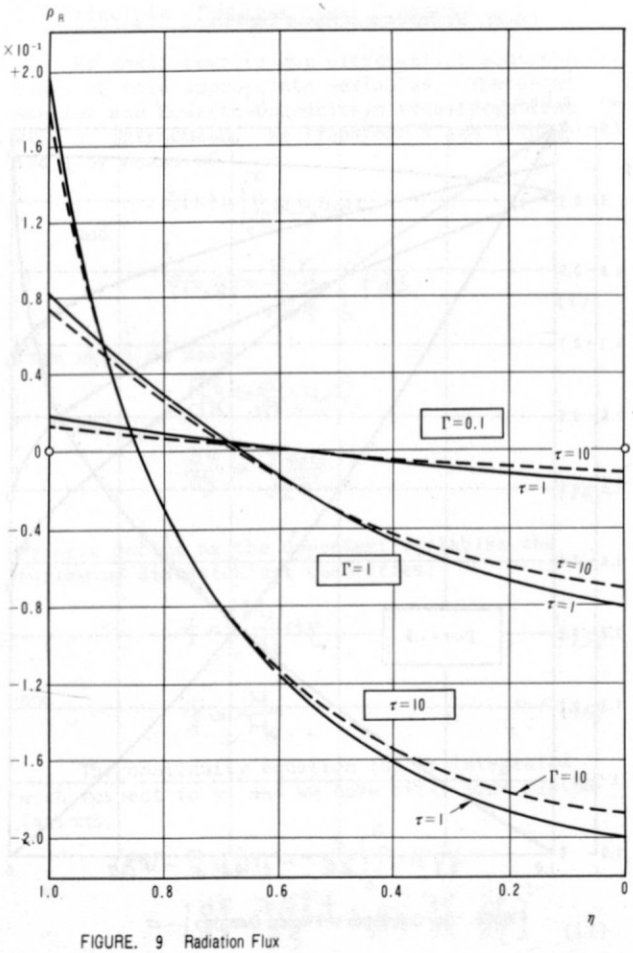

FIGURE. 9 Radiation Flux

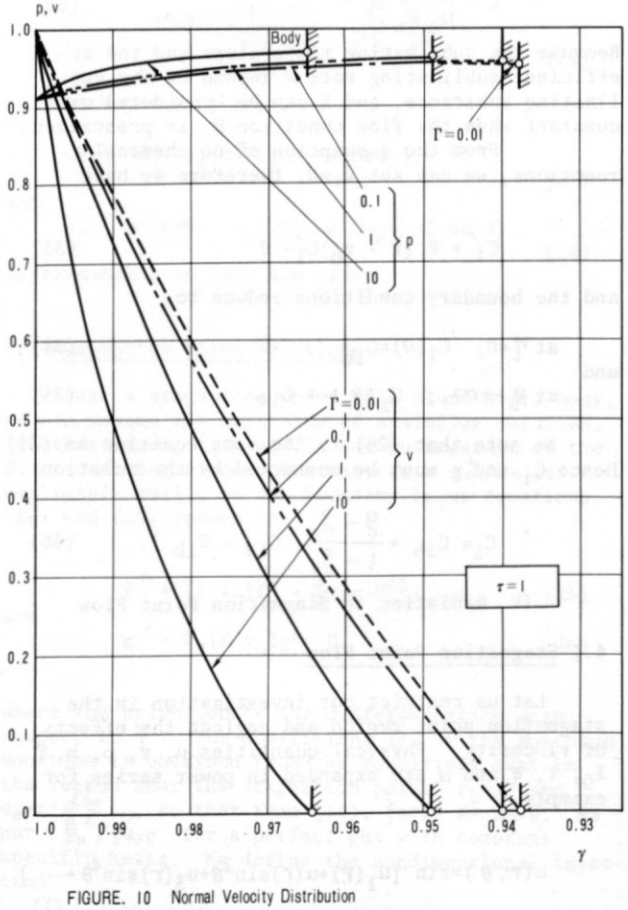

FIGURE. 10 Normal Velocity Distribution

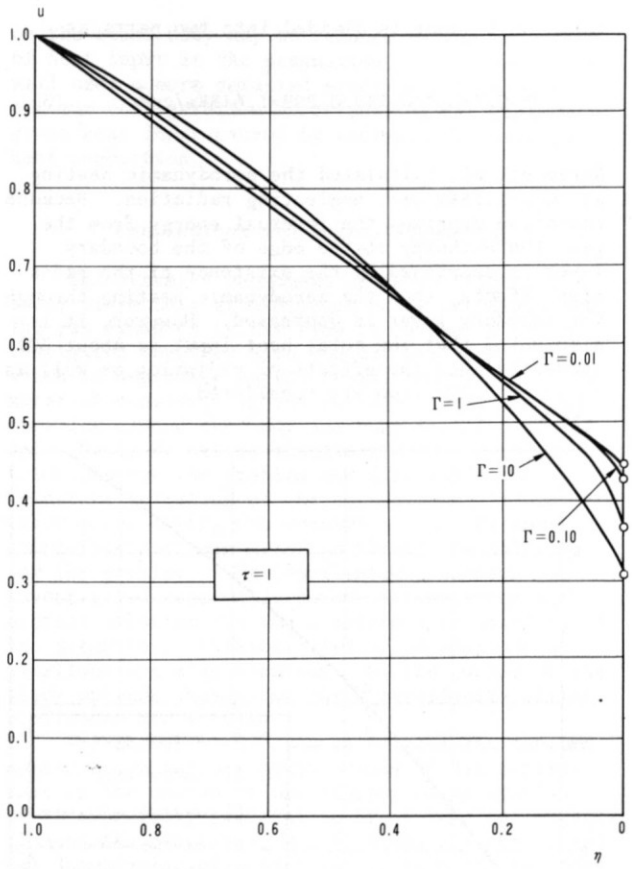

FIGURE. 11 Tangential Velocity Distribution

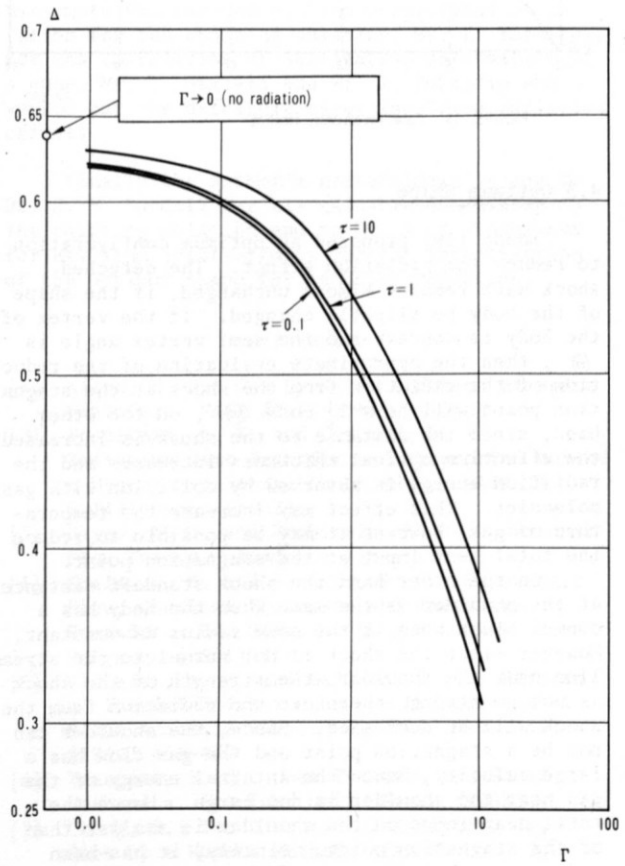

FIGURE. 12 Shock Standoff Distance

compared more clearly on the Fig 13. Enthalpy is higher whenever τ is larger.

Pressure distribution is given by

$$P_b = \cos^2\theta\,(0.947 - 0.361\sin^2\theta - 0.361\sin^4\theta + \cdots) \tag{2}$$

while the Newton's theory is $P_b = \cos^2\theta\ 0.947$. Theoretical results are compared with the experimental data at $M_\infty \doteqdot 5$ on Fig 14. At the hypersonic speed $M_\infty \gg 5$, the flow characterictics is almost unchanged by increasing of Mach number. This is the Mach independence principle.

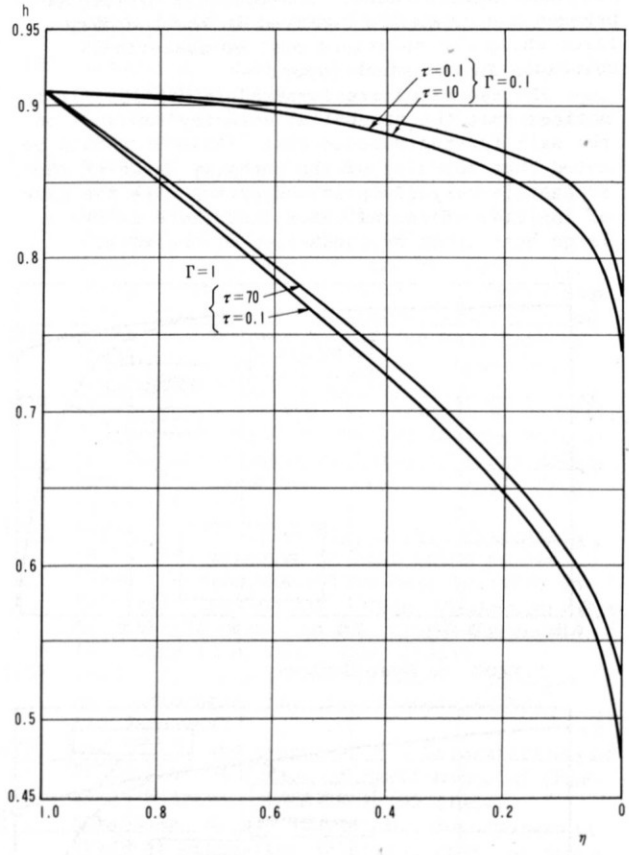

FIGURE. 13 Enthalpy Distribution

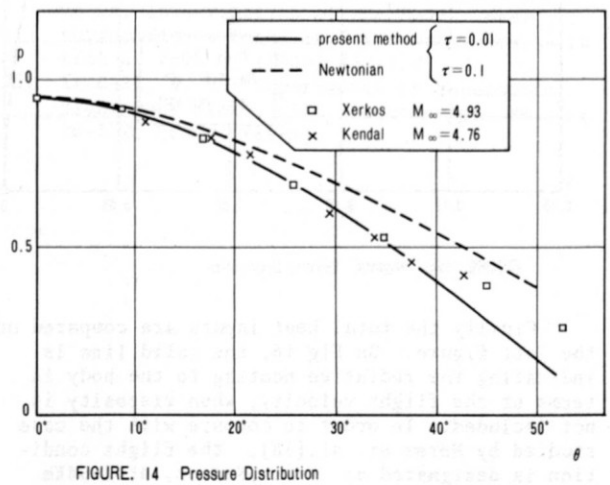

FIGURE. 14 Pressure Distribution

4.2 Effects of Viscosity

In addition to the radiative heating, heat conduction and heat produced by the friction are included to increase the heat input. As is indicated in Fig 11, the tangential velocity can not vanish on the surface of the body if viscosity of the fluid is neglected. The solution is so much unstable that it would take a long computation time before finding the solution satisfying the conditions on the solid wall starting from the shock condition. A perturbation method is applied to estimate the effects if viscosity, starting from the invicid cases. Considerable differences between two cases are observed in the boundary layer while the solutions must be essentially coincides in the shock layer.

The two cases are compared in Fig 15. It is noticed that the tangential velocity vanishes on the wall for the viscous case. Also it should be noted that the slop of the enthalpy curve at the surface is very steep in comparison with the case of invicid. This indicates that there exists a large heat input by conduction on the wall.

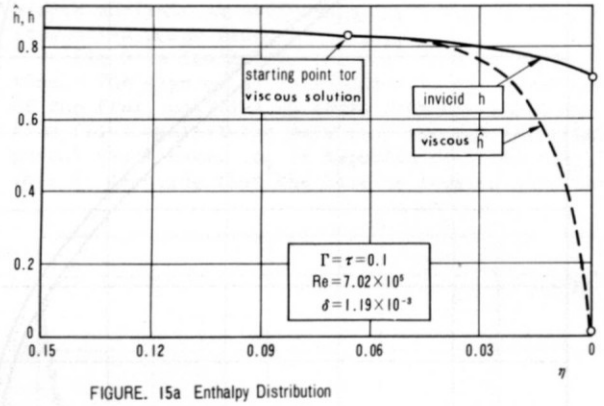

FIGURE. 15a Enthalpy Distribution

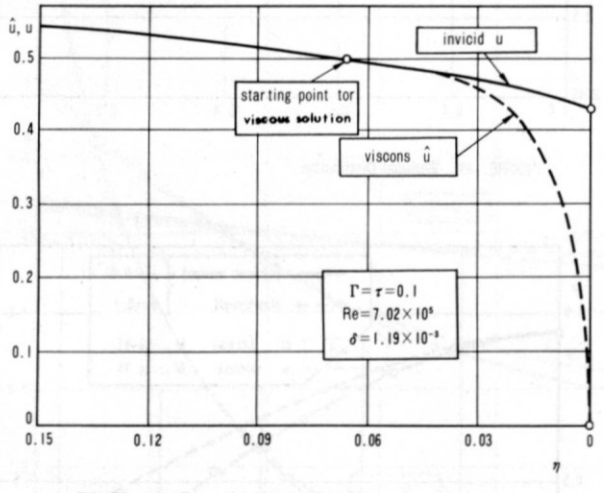

FIGURE. 15b Tangential Velocity Distribution

Finally the total heat inputs are compared on the last figure. On Fig 16, the solid line is indicating the radiative heating to the body in terms of the flight velocity, when viscosity is not included. In order to compare with the case studied by Nerem et. al.[18], the flight condition is designated as V=11.5Km/sec, at Z=54Km corresponding to $\Gamma = \tau = 0.1$ and R_N=1.5m. The total heat input is divided into two parts as

$$Q^* = Q_c^* + Q_R^* = 0.749 + 0.899 = 1.648 \text{Kw/cm}^2 \qquad (3)$$

Nerem et. al. calculated the aerodynamic heating as Q_{cr}=1.28Kw/cm^2, neglecting radiation. Because radiation deprives the interual energy from the gas, the enthalpy at the edge of the boundary layer is decreased by the existence of the radiation effects, thus the aerodynamic heating through the boundary layer is decreased. However, it is also noted that the total heat input is about 30% increased when the effects of radiation as well as those of conduction are considered.

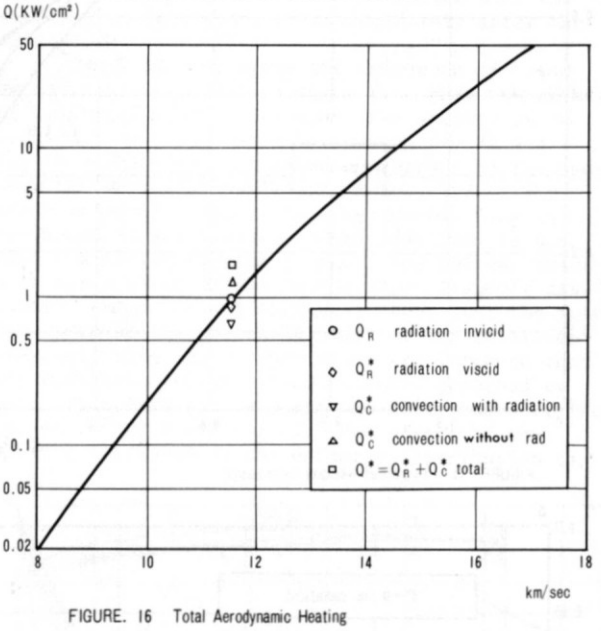

FIGURE. 16 Total Aerodynamic Heating

4.3 Optimum Shape

Kondo [19] proposed an optimum configuration to reduce the radiation effect. The detached shock wave remains almost unchanged, if the shape of the body be slightly changed. If the vertex of the body is concave and the semi vertex angle is Θ , then the approximate evaluation of the reduction of the radiation from the shock at the stagnation point will be $\sigma T_s^4 \cos^2 \Theta$, on the other hand, since the distance to the shock is increased the effective optical thickness increases and the radiation energy is absorbed by collision with gas molecules. This effect may increase the temperature of gas, however it may be possible to reduce the total heat input at the stagnation point.

On the other hand the shock standoff distance at the shoulder is the same when the body has a convex blunt nose if the nose radius is constant. However since the shock is not normal to the stream line near the shoulder, the strength of the shock is not so strong, therefore the radiation from the shock will be decreased. Since, the shoulder can not be a stagnation point and the gas flow has a large velocity, hence the internal energy of the gas near the shoulder is not large. Hence the total heat input on the shoulder is smaller than of the stagnation point. Finally, it has been understood that the peak of the total heat input

on the blunt body may be reduced by the reduction of heat input at the stagnation point, however it will need a more detailed study to determine the optimum configuration corresponding the minimum gross heat input caused by radiation as well as heat conduction.

Conclusions and Acknowledgements

Gas dynamics phenomena on space flight or reentry trajectory at a hypervelocity are discussed. The gas dynamics in the flow field should be investigated together with the surface condition which is depending on the termal properties of the material constructing the vehicle. Thus the gas dynamics around the body and heat transfer in the body should be solved simultaneously. Unsteady solutions for the problem are expected since a transient variation of the boundary conditions takes place during the reentry stage. Various simplifications are tried to obtain the solution for the problem. The complicated phenomena are investigated separately before we construct an overall solution for the complete understanding of the situation. Possibilities of several approximations are also examined. In the course of the study optimum shapes for the hypervelocity flight conditions are studied.

The author would like to express his sincere appreciation for the conjunctions of his colleagues in the course of the present investigation. He is especially grateful to Dr. S Tuge for suggestion of the existence, Mr. K. Koura for the numerical computation of a similar solution for the heat flow in graphite, Dr. T. Fujiwara and Mr. T. Matsumoto who carried out the complicated computation for the charring ablation, Mr. K. Yoshiyuki for the calculation of sublimating deformation of a cone, Mr. T. Okazaki and Mr. T. Tokairin who worked out the difficult cases involving radiation effects.

Finally the author's gratefulness is due to Dr. J. H. Lundell for his valuable discussion on the charring ablation and to Dr. K. K. Yoshikawa for his kind joint-efforts for the investigation of the optimum shape for reducing radiation.

References

[1] Allen, H. J.: Gas Dynamics Problems of Space Vehicles. NASA SP-11-2 Nov. (1962)

[2] Yoshikawa, K. K. and Chapman, D. R.: Radiative Heat Transfer and Absorption behind a Hypersonic Normal Shock Wave. NASA TN D-1424 Sept. (1962)

[3] Hayes, W. D. and Probstein, R. F.:Hypersonic Flow Theory. Academic Press (1966)

[4] Scala, S. M. and Sampson, D. H.: Supersonic Flow, Chemical Processes and Radiative Transfer. Ed. Olfe, D. B. and Zakkay, V. Pergamon (1964) 319

[5] Vincenti, W. G. and Baldwin, B. S.: Effects of Thermal Radiation on the Propagation of Plane Acoustic Waves. J. Fluid Mech. XII (1962) 449-477

[6] Traugott, S. C.: Heat Transfer and Fluid Mechanics, Stanford Univ. Press (1963)

[7] Cheng, P.: Two Dimensional Radiating Gas Flow by a Moment Method. AIAA J. Vol. 2, No. 9, Sept. (1964), 1662-1664

[8] Viegas, J. R. and Howe, J. T.: Thermodynamics and Transport Properties Correlation Formulas for Equilibrium Air from 1,000K to 15,000K. NASA TN D-1429 (1962)

[9] Hirschferder, J. O., Curtiss C. F. and Bird, R. B.: Molecular Theory of Gases and Liquid. John Wiley (1954)

[10] Bird, R. B., Stewart, W. E. and Lightfood, E.N.: Transport Phenomena. John Wiley (1960)

[11] Diaconis, N. W., Gorsuch, P. D. and Sheridan, R. A.: The Ablation of Graphite in Dissociated Air.Experimental Investigation. G. E. TIS R62SD72 (1962)

[12] Scala, S. M.: The Ablation of Graphite in Dissociated Air, Part I. Theory. G. E. TIS R62SD72 (1962)

[13] Nomura, S.: Measurement of Unsteady Aerodynamic Heating at Stagnation Region including Surface Reaction. J. Japan Soc. Aero/ Space Sci. XVI (1968) (in Japanese)

[14] Swann, R. T. and Pittman, C. M.: One-Dimensional Numerical Analysis of the Transient Response of Thermal Protection Systems. NASA TN D-2976 (1962)

[15] Kondo, J., Fujiwara, T. and Matsumoto, T.: Steady State Ablation of Charring Materials. Proc. VII I. S. T. S. (Tokyo, 1967) 351-360

[16] Kondo, J.: Deformation of the Nose Cone by Sublimating Ablation. Trans. Japan Soc. Aero/Space Sci. V (1962) 69-74

[17] Kondo, J., Yoshizawa, Y., Suzuki, K. and Sato, J.: Determination of the Sublimating Rate at the Forward Stagnation Point of Blunt Bodies. Proc. 11th Japan Nat. Cong. for Appl. Mech. (1961) 167-173

[18] Nerem, R. M., Stickford, G. H.: Stagnation Point Heat Transfer in High Enthalpy Gas Flows. Part I: Convective Heat Transfer in Partially Ionized Air. Tech. Documentary Rpt. No. FDL-TDR-64-41, pt. I, Wright-Patterson Air Force Base, Ohio, Mar. (1964)

[19] Kondo, J.: Reentry Aerodynamics. J. Japan Soc. Aero/Space Sci. XIV (1966) 183-191 (in Japanese)

[20] Dow, M. B. and Swann, R. T.: Determination of Effects of Oxidation on Performance of Charring Ablators. NASA TR R-196 (1964)

[21] Karashima, K. amd Kubota, H.: Aerodynamic Study of Stagnation Ablation. Inst. of Space and Aeronautical Sci., Univ. Tokyo, Rpt. No. 413 June (1967) 87-119

[22] Xerikos, J. and Anderson, W. A.: An Experimental Investigation of the Shock Layer surrounding a Space in Supersonic Flow. AIAA J. Vol. 3, (1965) 451-457

[23] Kendall, J. M.: Experiments on Supersonic Blunt Body Flows. JPL Progress Rpt. No. 20-372, Calif. (1959)